Cold QCD physics with STAR at RHIC

B.E. Aboona, C.A. Gagliardi and the STAR Collaboration

Our group continues to play a major role in the STAR spin physics program. Over the past year, our analysis efforts have focused on three measurements: the Collins effect in 200 GeV p+Au collisions, the Collins effect in 510 GeV pp collisions, and an investigation of the contribution from diffractive processes to the large transverse single-spin asymmetry, A_N, that is seen for forward rapidity electromagnetic jets (EM-jets) in 200 GeV pp collisions. In addition, group members have continued to carry a wide range of administrative responsibilities for STAR.

Our graduate student B. Aboona is analyzing data that STAR recorded during 2015 to determine the size of the Collins effect in $\sqrt{(s_{NN})}$ = 200 GeV p+Au collisions. This will provide unique insight into the possible factorization breaking that has been predicted for transverse-momentum-dependent phenomena in hadronic collisions, in addition to a spin-dependent probe of the hadronization mechanism in cold nuclear matter.

High-quality particle identification (PID) is an important step in the Collins analysis. It requires a detailed understanding of the response of the PID quantities commonly used in STAR analyses. PID from the time projection chamber (TPC) is obtained using a quantity known as n_σ. This quantity returns the difference between the measured and the calculated dE/dx of a track in units of resolution, σ. For example, a reconstructed track whose $n_\sigma(\pi)$~0 is very likely to be a pion. Each track has four n_σ values: $n_\sigma(\pi)$, $n\sigma(K)$, $n_\sigma(p)$, and $n_\sigma(e)$. Similarly, PID from the time of flight (TOF) system is obtained using $n_{\sigma,TOF}$. Here, the quantity returns the difference between the measured and the calculated TOF of a given track divided by the TOF resolution. Eqs 1 and 2 summarize the model functions for n_σ and $n_{\sigma,TOF}$, respectively, where the details of how these functional forms have been obtained are discussed in last year's report. A two-dimensional functional form can be achieved by the product of $g(x)$ and $h(y)$, which results in a functional form where b, α, μ_2, and σ_2 are constants.

$$g(x) = Ae^{-\frac{1}{2}\left[\frac{x-\mu}{\sigma+b(x-\mu)}\right]^2} \qquad (1)$$

$$h(y) = A_1\left[e^{-\frac{1}{2}\left(\frac{y-(\langle y\rangle-0.085)}{\sigma_1}\right)^2} + \alpha e^{-\frac{1}{2}\left(\frac{y-(\langle y\rangle-0.085+\mu_2)}{(\sigma_1+\sigma_2)}\right)^2}\right] \qquad (2)$$

We produce momentum (p) and pseudorapidity (η) binned two-dimensional histograms of $n_\sigma(\pi, K, p)$ vs. $n_{\sigma,TOF}(\pi, K, p)$ for all the tracks in jets of interest to our analysis and utilize the two-dimensional functional model to fit the histograms. Fig. 1 is a sample two-dimensional fit. The p and η binning results in 2880 two-dimensional histograms, each requiring a two-dimensional likelihood fit with 15 or 20 free parameters. These multi-peak, two-dimensional likelihood fits are computationally intensive, and some can be unstable. Optimization steps have been implemented to address these issues.

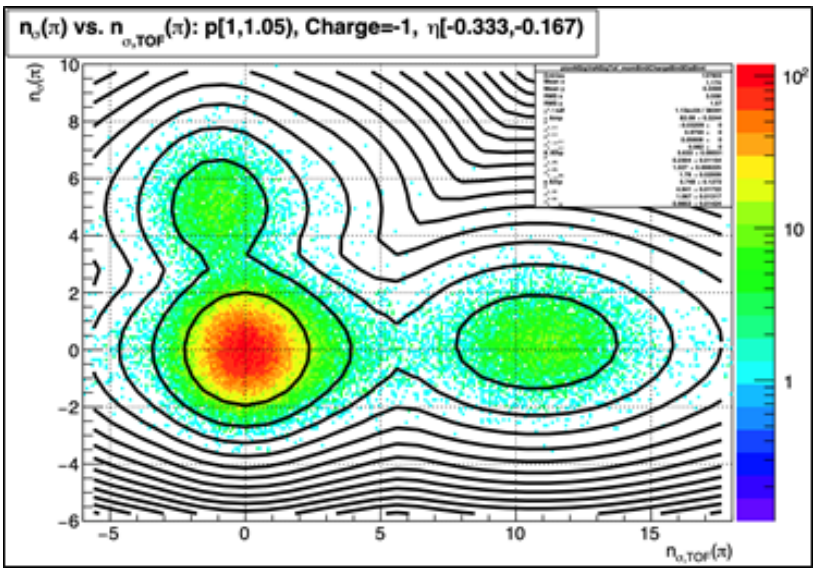

FIG. 1. A sample fitted $n_\sigma(\pi)$ vs. $n_{\sigma,TOF}(\pi)$ distribution in the momentum range $1 < p < 1.05$ GeV/c and $\boldsymbol{\eta}$ range $-0.33 < \eta < -0.167$. At this momentum, the proton peak is far off the right-hand side of the plot.

We analytically calculate the $n_{\sigma,TOF}$ mean difference between two particle peaks. This is made possible by knowing the mean p and η of the particle species, as well as the geometry of the STAR detector. We then compare the analytical calculations to the $n_{\sigma,TOF}$ mean differences from data. Fig. 2a illustrates the good agreement between the analytical calculations and data. Given that pions are the highest statistic peak, we utilize the calculated $n_{\sigma,TOF}$ mean differences to fix the $n_{\sigma,TOF}$ means of K, p, and e with respect to the pion peak, thus reducing the number of free parameters in the fit.

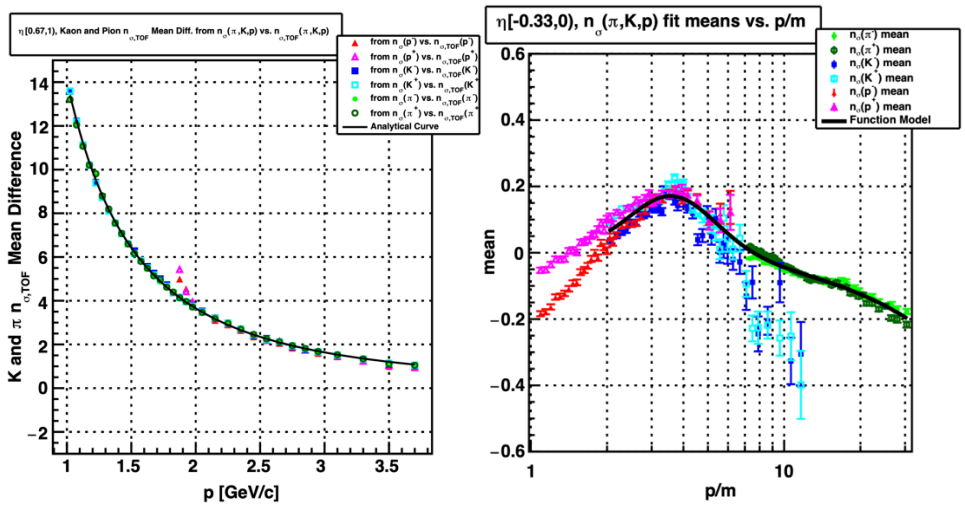

FIG. 2. (a) Data points show the difference between the $\boldsymbol{K}$ and $\boldsymbol{\pi}$ $\boldsymbol{n_{\sigma,TOF}}$ means from data, and the black curve shows the result of calculating the difference analytically. (b) Data points are the means of $\boldsymbol{n_\sigma(\pi, K, p)}$ vs. $\boldsymbol{p/m}$ from data, and the black curve shows the result of the model fit function.

We further reduce the number of free parameters in the fits by modeling the means and sigmas of n_σ and $n_{\sigma,TOF}$ for the signal peak in each fit. As an example to illustrate this point, Fig. 2b shows the mean of $n_\sigma(\pi, K, p)$ vs. p/m, where m is the respective particle mass. The black curve is a model function that fits the data above $p/m \sim 2$. This model function is then used to analytically calculate the mean of $\pi, K,$ and p for a given value of p/m when $\pi, K,$ and p are the signal peaks during the fitting process. The region below $p/m = 2$ corresponds to well-isolated protons, and therefore only a single peak needs to be fitted and model calculations are unnecessary there.

Using information from the two-dimensional fits, we can calculate particle fractions for a given p and η bin by calculating the ratio of integrated particle yields (A_i). Eq. 3 shows an example of how A_π can be calculated, where N_i is the integral of the two-dimensional fit function using the appropriate parameters for the respective particle peak in a given kinematic bin and $i = \pi,\ K,\ p,$ or e. The focus particle of each two-dimensional fit can be any one of the four particle species. A sample comparison between the kaon yield for "pion-centric" versus "kaon-centric" fits is shown in Fig. 3. Below ~2 GeV/c, both the pion-centric and kaon-centric A_K values are similar. Beyond ~2 GeV/c, A_K values from the kaon-centric two-

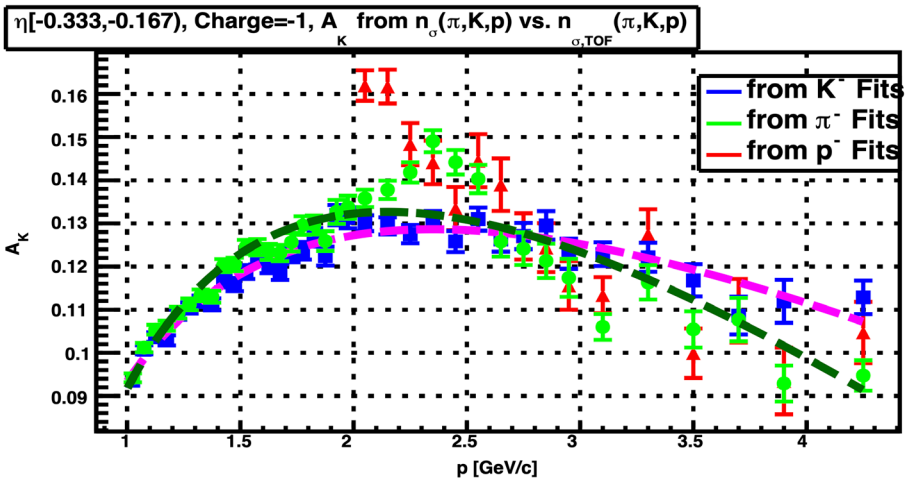

FIG. 3. Comparison between "kaon-centric" and "pion-centric" $\boldsymbol{A_K}$ yields, each of which is fitted with a model function.

dimensional fits are more "well-behaved" when compared to the pion-centric A_K values. This stems from the difference between how the pion and kaon fits are handled. In the pion-centric fit, all the fit parameters for the pion peak are fixed except for the amplitude. The $n_{\sigma,TOF}(K)$ mean is determined with respect to the $n_{\sigma,TOF}(\pi)$ peak, which allows the kaon peak to be easier to fit, but it is still challenging at higher momenta. On the other hand in a kaon-centric fit, all fit parameters for the kaon peak are fixed except for the amplitude, which makes the job of the fitter easier, especially at higher momenta. All parameters corresponding to the pion peak are free, but the pion peak is the highest statistic peak and the fitter is able to locate it easily. Therefore, these differences between the ways the fits are handled lead to the different A_K values between the two fits. We have adopted the fractional yields from kaon-centric fits for the Collins PID procedure. The difference between the kaon-centric and pion-centric yields is assigned as the systematic uncertainty associated with PID.

$$A_\pi = \frac{N_\pi}{N_\pi + N_K + N_p + N_e} \qquad (3)$$

During 2017, STAR recorded a transversely polarized *pp* dataset at $\sqrt{s}$ = 510 GeV with 16 times the figure of merit of the previous measurement [1]. Fig. 4 shows a comparison of the preliminary Collins asymmetries found in the 2017 data with our previous measurements in 200 GeV *pp* collisions [2]. No energy dependence is observed within uncertainties. This sets a stringent limit on evolution effects for transverse-momentum-dependent fragmentation functions. A paper describing these results is being written at present, with Dr. Gagliardi as one of the five principal authors.

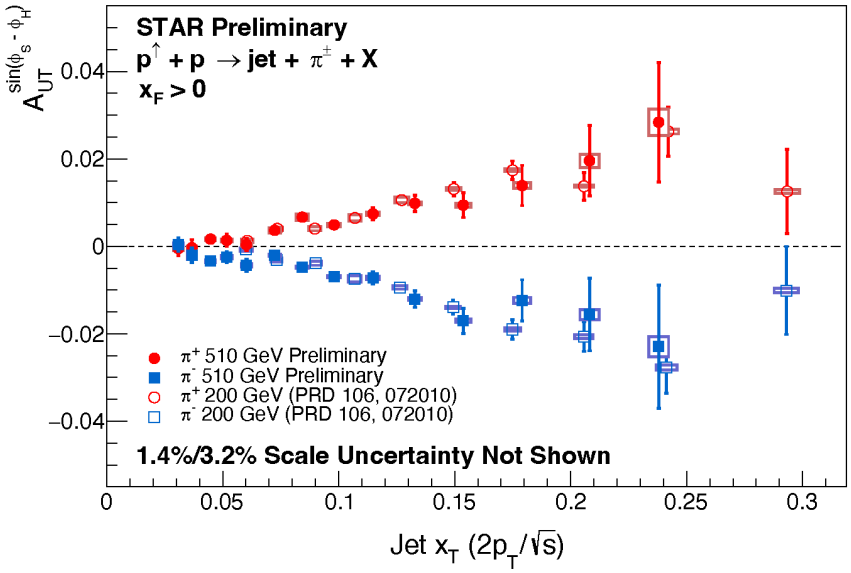

FIG. 4. Comparison of preliminary STAR Collins asymmetry measurements in 510 GeV *pp* collisions with previous results from 200 GeV *pp* collisions [2].

Recently, STAR published measurements of forward π^0 and EM-jet A_N [3] that indicate the large transverse single-spin asymmetries that have been seen for inclusive hadron production at forward rapidities are unlikely to arise from either the Collins or Sivers effects. This led to the question whether the large asymmetries might arise from diffractive processes. The UC-Riverside group began a study of EM-jets observed in *pp* data at $\sqrt{s}$ = 200 GeV that STAR recorded during 2015 to explore this question, and asked Dr. Gagliardi to join the effort. Two different processes have been investigated. In one case, A_N has been measured for the case where a moderate to high-p_T EM-jet and a low-p_T, near-beam momentum proton are both observed at forward rapidity, with the summed energy of the EM-jet and proton consistent with the initial beam energy. The observed asymmetry is found to be negative, which is opposite in sign to the inclusive EM-jet asymmetry. In the other case, EM-jets that arise from single diffraction are being studied by measuring the probability that beam-like protons are seen in the opposite hemisphere. In this case, the observed spin asymmetries are consistent within statistics with those for EM-jets from non-diffractive collisions. Two papers are being written at present. The first will provide a detailed multi-dimensional (x_F,

p_T, photon multiplicity) map of the inclusive EM-jet asymmetries over the pseudo-rapidity range $1 < \eta < 4$. The other will report the comparison of the spin asymmetries found for diffractive processes with those for inclusive EM-jets. Dr. Gagliardi is one of the seven principal authors for both papers.

Finally, we continue to carry various administrative responsibilities for STAR. Dr. Gagliardi was a member of the Trigger Board for Run 23, and is serving again for Run 24. He served as the chair of the god-parent committee for one publication [4] and as a member of the god-parent committee for four others [5-8]. He also made important, but informal, contributions to three other STAR papers [9-11]. In parallel, Mr. Aboona has served as the code-QA representative on the god-parent committee for one paper [9].

[1] L. Adamczyk *et al*. (STAR Collaboration), Phys. Rev. D **97**, 032004 (2018).
[2] M.S. Abdallah *et al*. (STAR Collaboration), Phys. Rev. D **106**, 072010 (2022).
[3] J. Adam *et al*. (STAR Collaboration), Phys. Rev. D **103**, 092009 (2021).
[4] M.I. Abdulhamid *et al*. (STAR Collaboration), Phys. Rev. D **109**, 012004 (2024).
[5] M.I. Abdulhamid *et al*. (STAR Collaboration), JHEP **06**, 176 (2023).
[6] STAR Collaboration, Phys. Rev. C (2023) (submitted); arXiv:2309.00145.
[7] STAR Collaboration, Phys. Rev. Lett. (2023) (submitted); arXiv:2309.00156.
[8] STAR Collaboration, Nature (2023) (submitted); arXiv:2310.12674.
[9] STAR Collaboration, Phys. Rev. Lett. (2023) (submitted); arXiv: 2305.10359.
[10] STAR Collaboration, Phys. Rev. Lett. (2023) (submitted); arXiv:2311.13637.
[11] STAR Collaboration, Phys. Rev. C (2023) (submitted); arXiv:2311.13632.